



# Società Italiana di Fisica 101° Congresso Nazionale

Roma 21 – 25 Settembre 2015

Numerical modeling and tomographic inversion for  
CO<sub>2</sub> monitoring in a saline aquifer

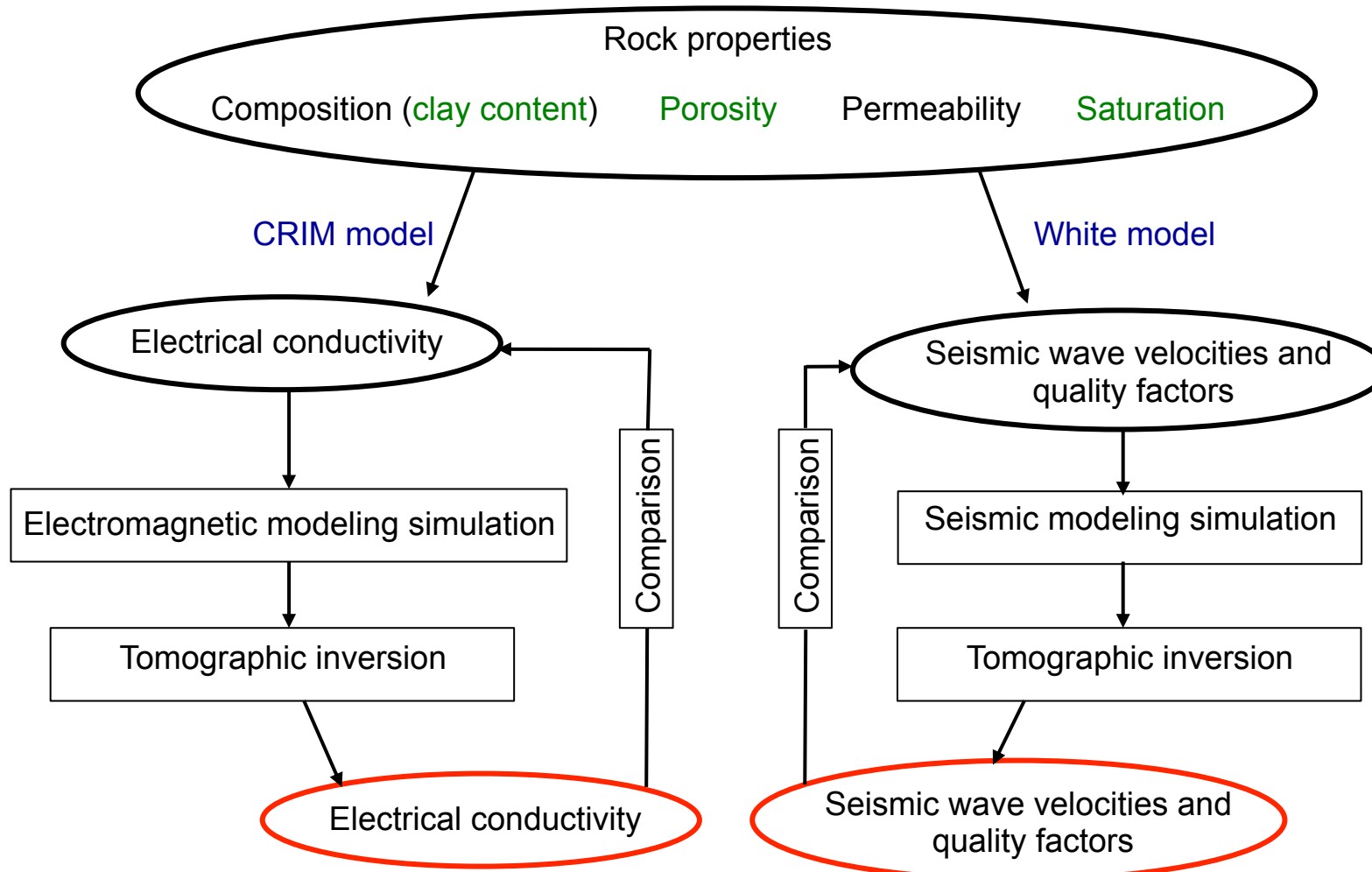
**Gei D.**, Carcione J., Bohm G., Picotti S., Michelini A., Currenti G.



# Methodology

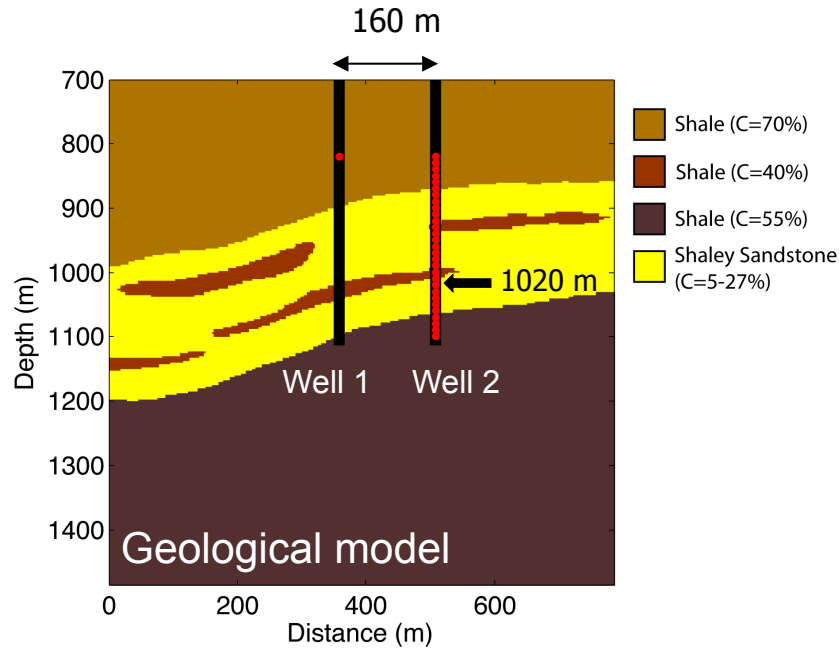


We present an combined rock-physics methodology of electromagnetic (EM) and seismic wave propagation for the detection and monitoring of CO<sub>2</sub> in cross-well experiments.

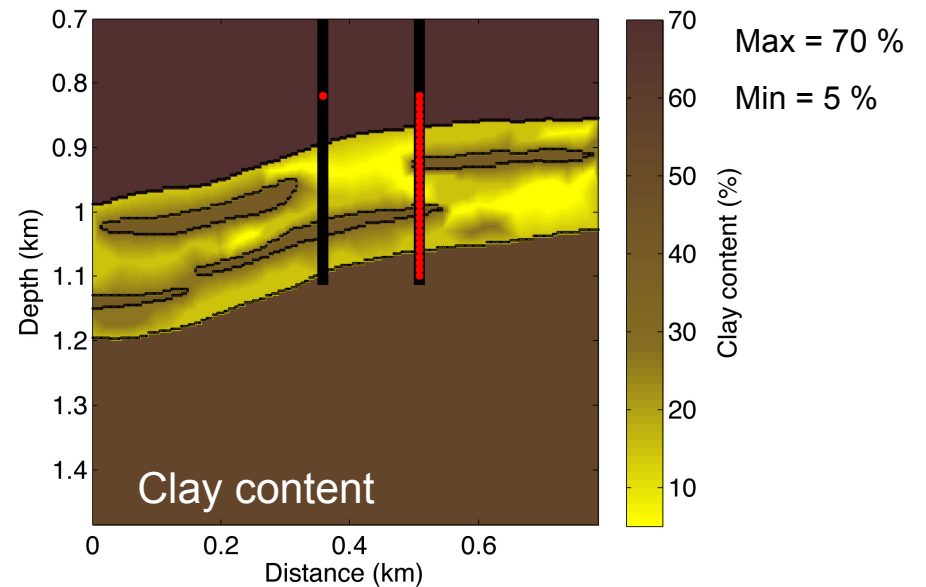
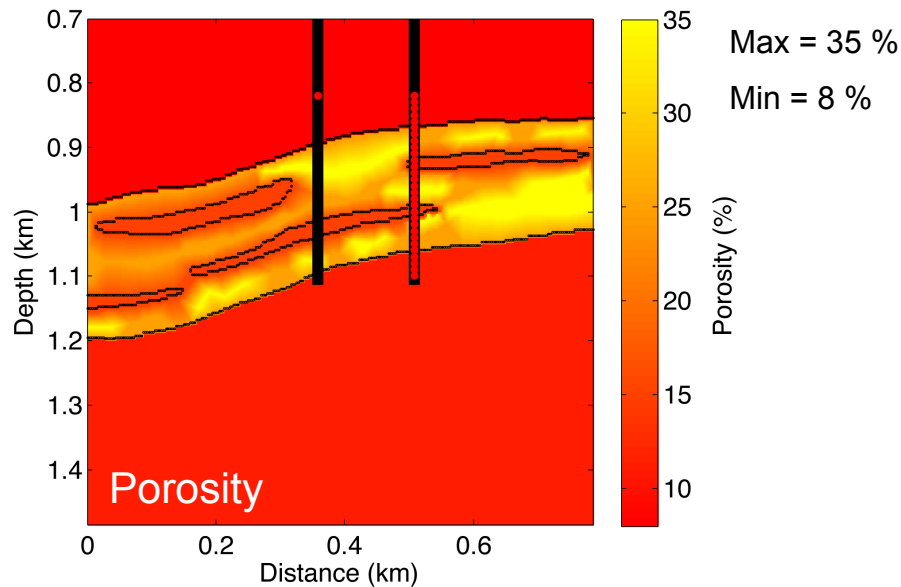




# Assumed models

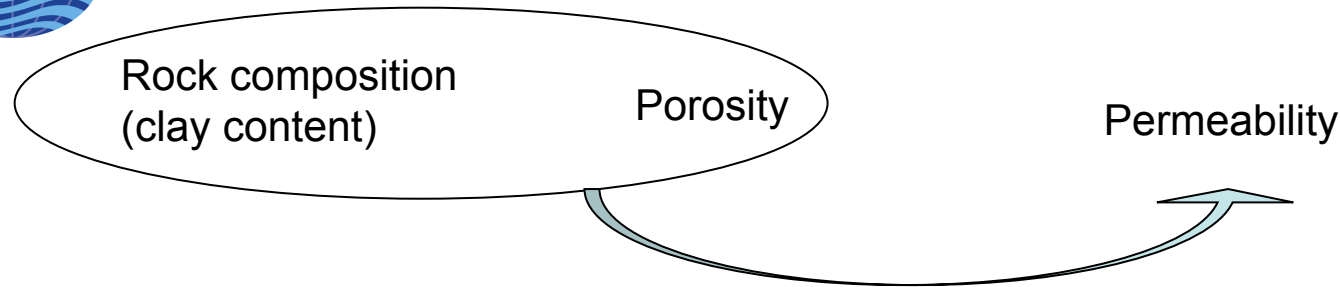


Aquifer depth: 900 – 1200 m  
Aquifer thickness:  $\approx$  200 m  
Well 1: 15 sources ( $dz = 20$  m)  
Well 2: injection and 29 receivers ( $dz = 10$  m)





# Permeability



$$\kappa_q = \frac{R_q^2 \phi^3}{45(1 - \phi)^2(1 - C)} \quad \kappa_c = \frac{R_c^2 \phi^3}{45(1 - \phi)^2 C}$$

$$\frac{1}{\kappa} = \frac{1 - C}{\kappa_q} + \frac{C}{\kappa_c} = \frac{(1 - \phi)^2}{A\phi^3} [(1 - C)^2 + C^2 B^2]$$

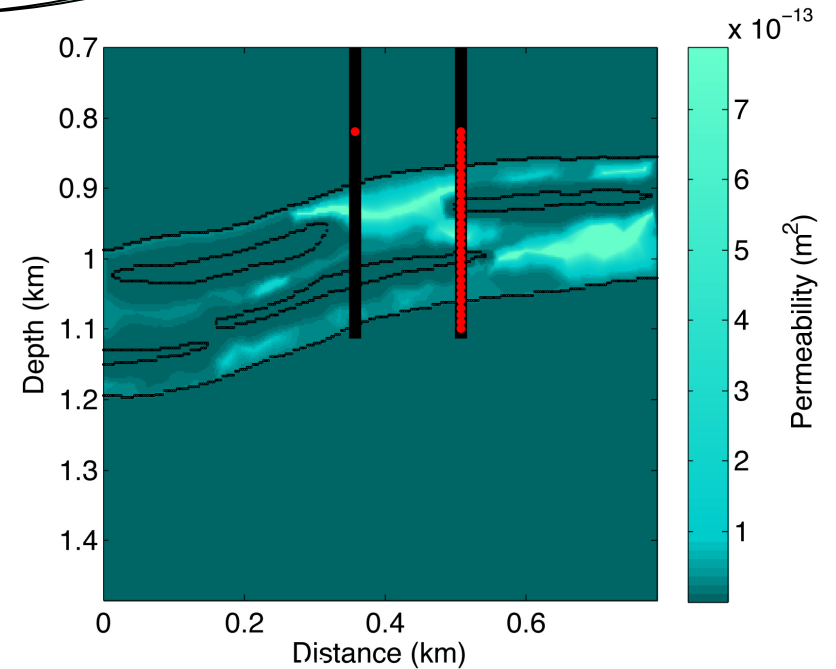
$$A = R_q^2/45 \quad B = R_q/R_c$$

$\kappa_q, \kappa_c$  = sandy and shaly matrices partial permeabilities

$R_q, R_c$  = average radii of sand and clay particles

$C$  = clay content

$\phi$  = porosity



Max = 7.8822e<sup>-13</sup> m<sup>2</sup>

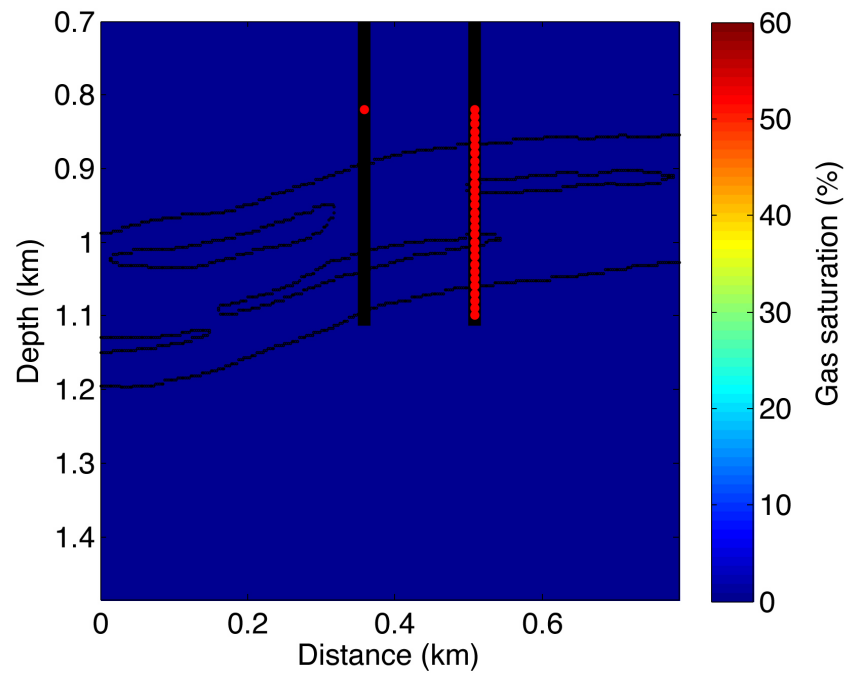
Min = 2.7432e<sup>-17</sup> m<sup>2</sup>



# Saturation

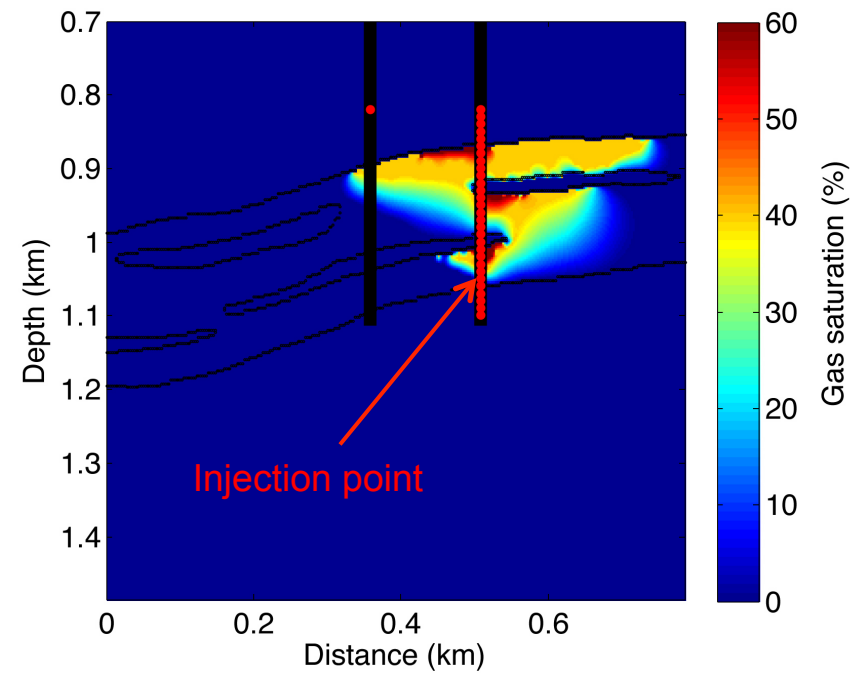


Gas saturation before CO<sub>2</sub> injection



Max = 0 %  
Min = 0 %

Gas saturation after CO<sub>2</sub> injection  
(assumed)



Max = 60 %  
Min = 0 %



# Conductivity



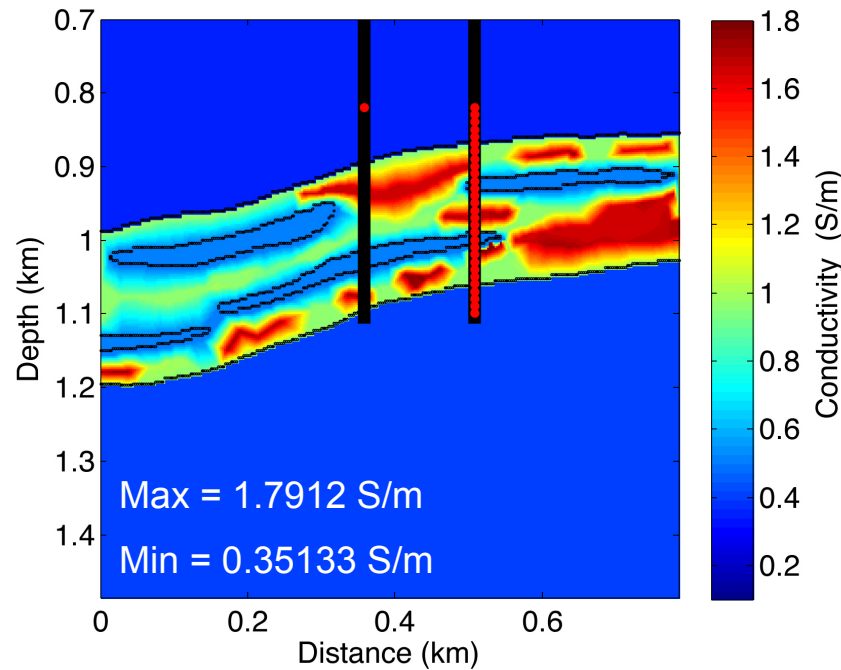
## Complex Refractive Index Method (CRIM)\*

Conductivity of a shaly sandstone with negligible permittivity and partially saturated with gas:

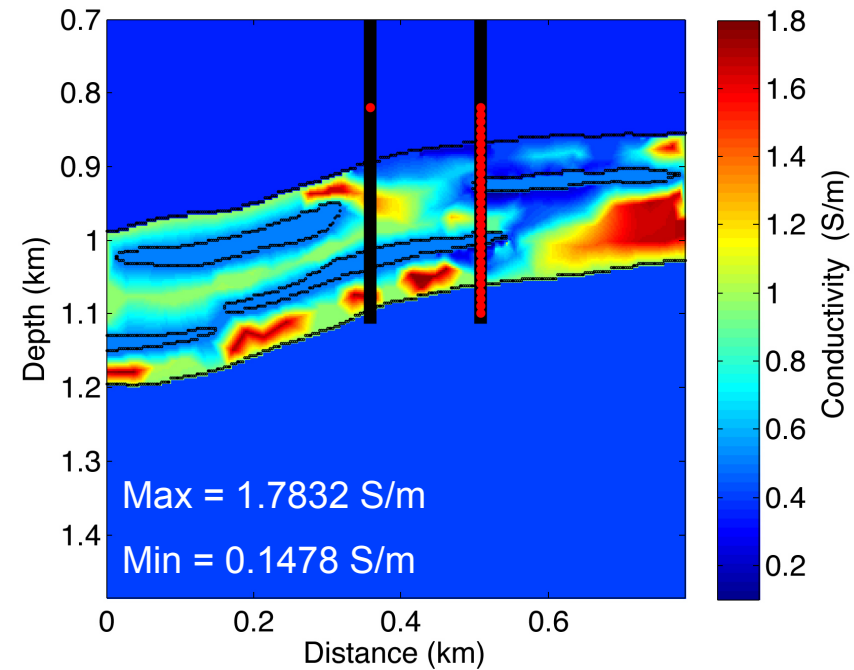
$$\sigma = [(1 - \phi)(1 - C)\sigma_q^\gamma + (1 - \phi)C\sigma_c^\gamma + \phi(1 - S_g)\sigma_b^\gamma + \phi S_g\sigma_g^\gamma]^{1/\gamma}, \quad \gamma = 1/2$$

- $C$  = clay content
- $S_g$  = gas saturation
- $\sigma_q$  = quartz conductivity
- $\sigma_c$  = clay conductivity
- $\sigma_g$  = gas conductivity
- $\sigma_b$  = brine conductivity
- $\phi$  = porosity

### Conductivity before CO<sub>2</sub> injection



### Conductivity after CO<sub>2</sub> injection



\*(e.g. Schön, 1996)



# Bulk density



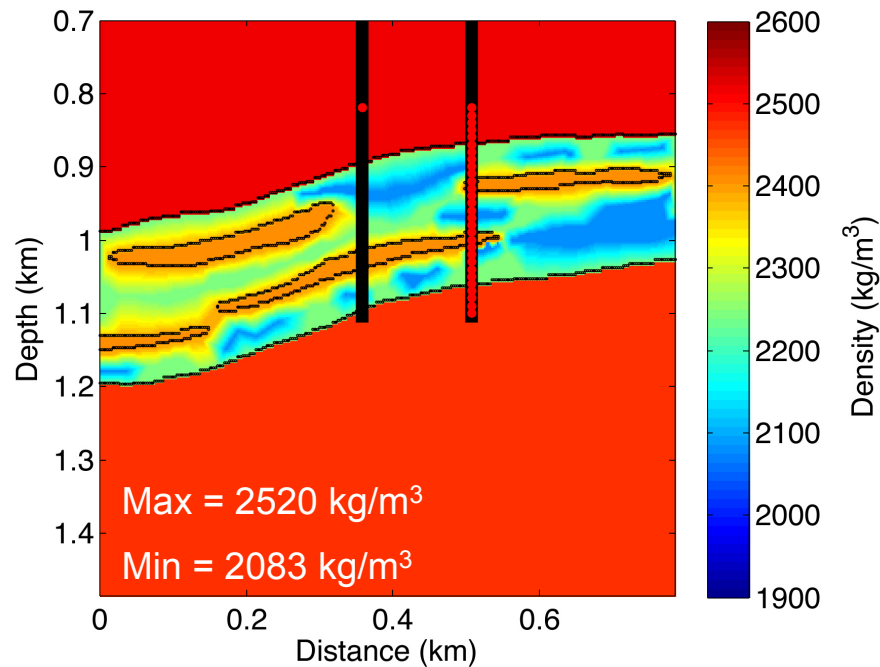
The density of a shaly sandstone partially saturated with gas can be computed with:

$$\rho_f = S_g \rho_g + (1 - S_g) \rho_b$$

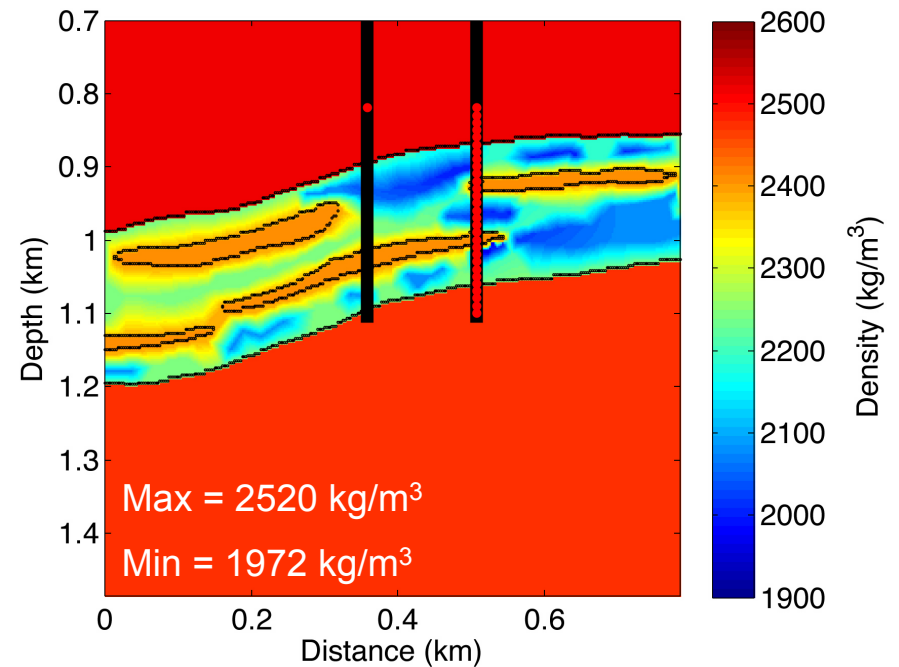
$$\rho = (1 - \phi)[(1 - C) \rho_q + C \rho_c] + \phi \rho_f$$

- $C$  = clay content
- $S_g$  = gas saturation
- $\rho_q$  = density of quartz particles
- $\rho_c$  = density of clay particles
- $\rho_g$  = density of gas ( $\text{CO}_2$ )
- $\rho_b$  = density of brine
- $\phi$  = porosity

Bulk density before  $\text{CO}_2$  injection



Bulk density after  $\text{CO}_2$  injection



Dry-rock bulk modulus (Krief model)

$$K_m = K_s(1 - \phi)^{A/(1-\phi)}$$

Dry-rock shear modulus (assumed)

$$\mu_m = \frac{\mu_s}{K_s} K_m$$

$K_m$  = dry rock bulk modulus

$\mu_m$  = dry rock shear modulus

$K_s$  = bulk modulus of the grains

$\mu_s$  = shear modulus of the grains

$\phi$  = porosity

$A = 3$

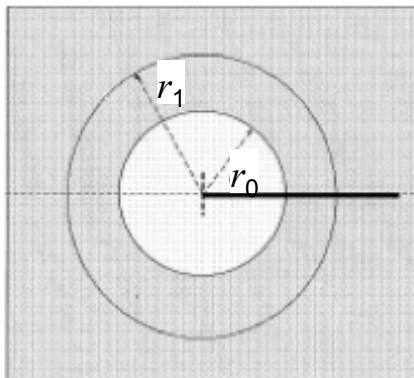
White model (1975) – patchy saturation

Complex bulk modulus as a function of frequency of a shaly sandstone partially saturated with gas:

$$K = \frac{K_\infty}{1 - K_\infty W}$$

$$W(f, r_0, r_1, \eta_g, \eta_b, \kappa, \phi, K_m, \mu_m, K_b, K_g, K_s)$$

$$K_\infty(r_0, r_1, \phi, K_m, \mu_m, K_b, K_g)$$



$$S_g = \frac{r_0^3}{r_1^3}$$

$\kappa$  = permeability

$K_m$  = dry rock bulk modulus

$\mu_m$  = dry rock shear modulus

$K_b$  = brine bulk modulus

$K_g$  = gas bulk modulus

$K_s$  = grains bulk modulus

$S_g$  = gas saturation

$f$  = frequency

$r_0$  = inner radius (gas patch)

$r_1$  = outer radius

$\eta_b$  = brine viscosity

$\eta_g$  = gas viscosity





# P- and S- wave velocities of saturated rocks



$$v_P = \sqrt{\left(K(f_0) + \frac{4}{3}\mu\right) / \rho} \quad V_P = \left[Re\left(\frac{1}{v_P}\right)\right]^{-1}$$

$$v_S = \sqrt{(\mu_m + i \mu_m / Q_\mu) / \rho} \quad V_S = \left[Re\left(\frac{1}{v_S}\right)\right]^{-1}$$

$K(f_0)$  = White complex bulk modulus

$\mu_m$  = dry rock shear modulus

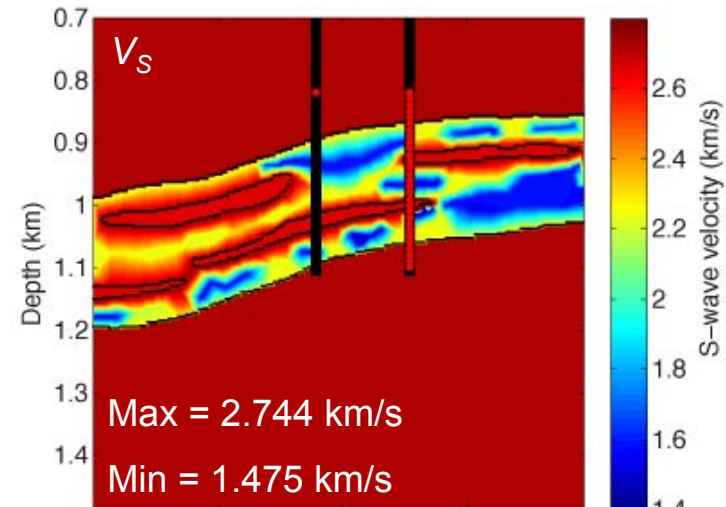
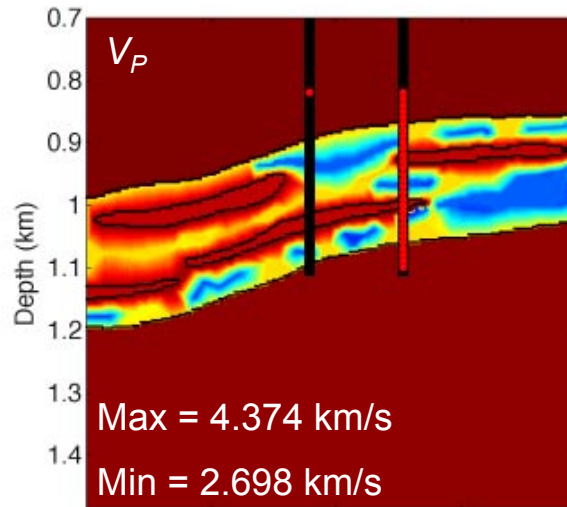
$\mu$  = complex shear modulus

$v_i$  = complex wave velocity (i=P, S)

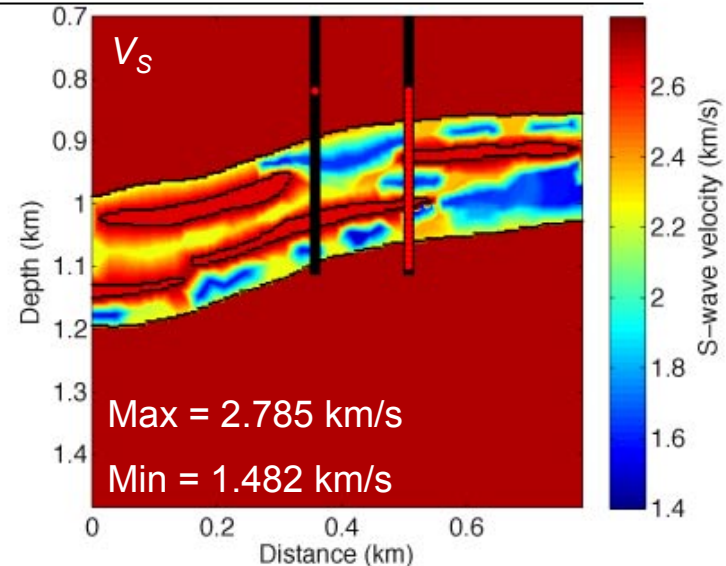
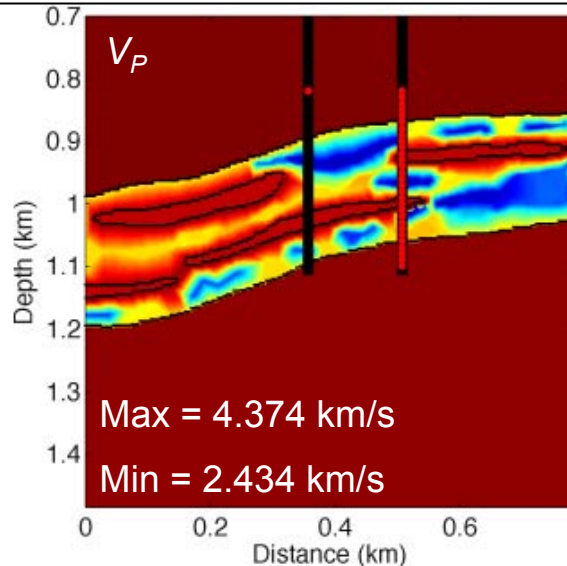
$V_i$  = real wave velocity (i=P, S)

$Q_\mu$  = shear quality factor

Before CO<sub>2</sub> injection



After CO<sub>2</sub> injection





# Quality factors of saturated rocks



$$Q_K = \frac{\text{Re}(K(f_0))}{\text{Im}(K(f_0))} \quad Q_\mu = \frac{\mu_m}{\text{Re}[K(f_0)]} Q_K$$

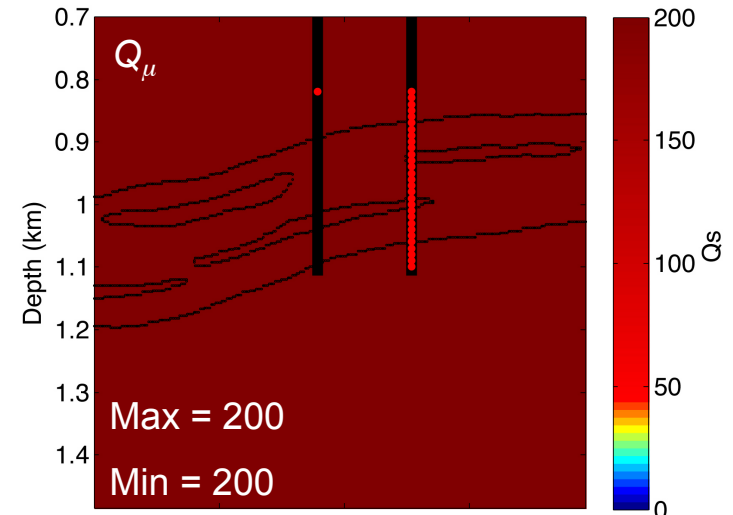
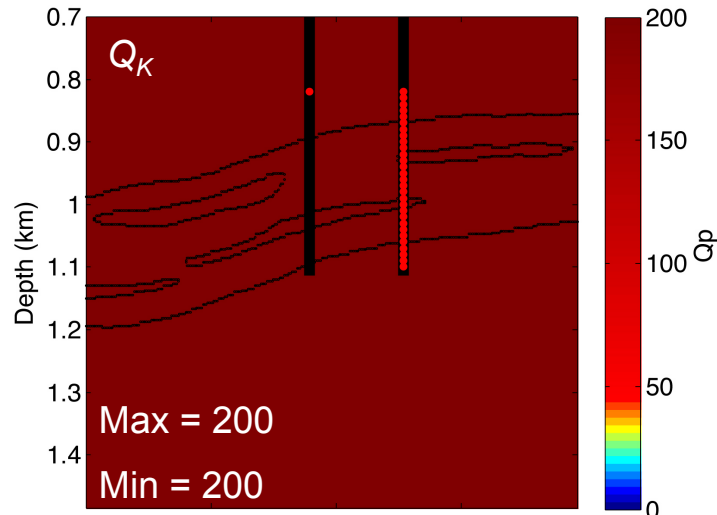
$K(f_0)$  = White complex bulk modulus

$\mu_m$  = dry rock shear modulus

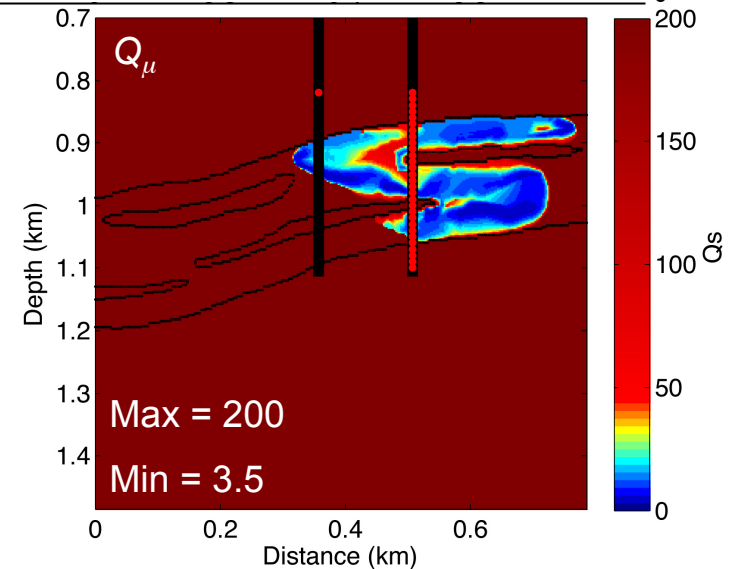
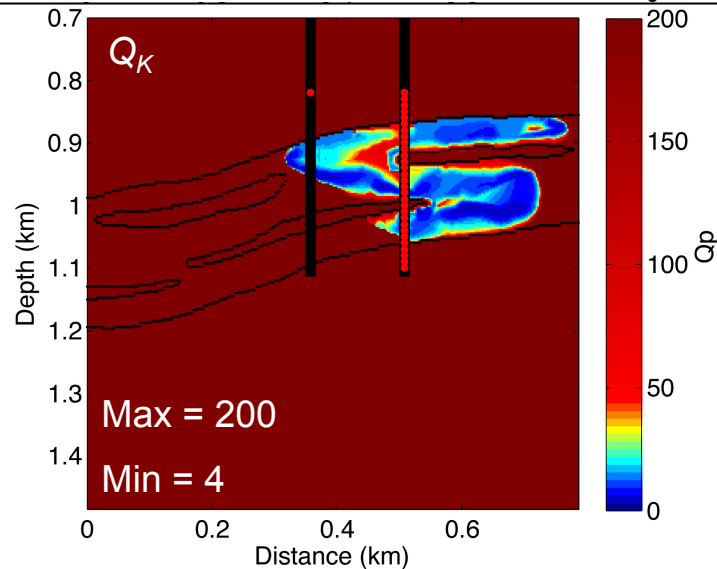
$Q_K$  = quality factor associated with  $K$

$Q_\mu$  = quality factor associated with  $\mu$

Before CO<sub>2</sub> injection



After CO<sub>2</sub> injection





## EM numerical modelling



TM (transverse magnetic) equation

$$\mu_0 \dot{H}_y = (\sigma^{-1} H_{y,x})_{,x} + (\sigma^{-1} H_{y,z})_{,z} - \mu_0 \dot{M}_y + (J_{x,z} - J_{z,x})$$

$\mu_0$  = magnetic permeability of vacuum

$H_y$  = magnetic field

$\sigma$  = electrical conductivity

$M_y$  = magnetic source

$J$  = electric sources

Regular grid (315 x 315; dx = dy = 2.5 m)

Spatial derivatives: pseudospectral (Fourier) method

Time evolution: Chebyshev expansion

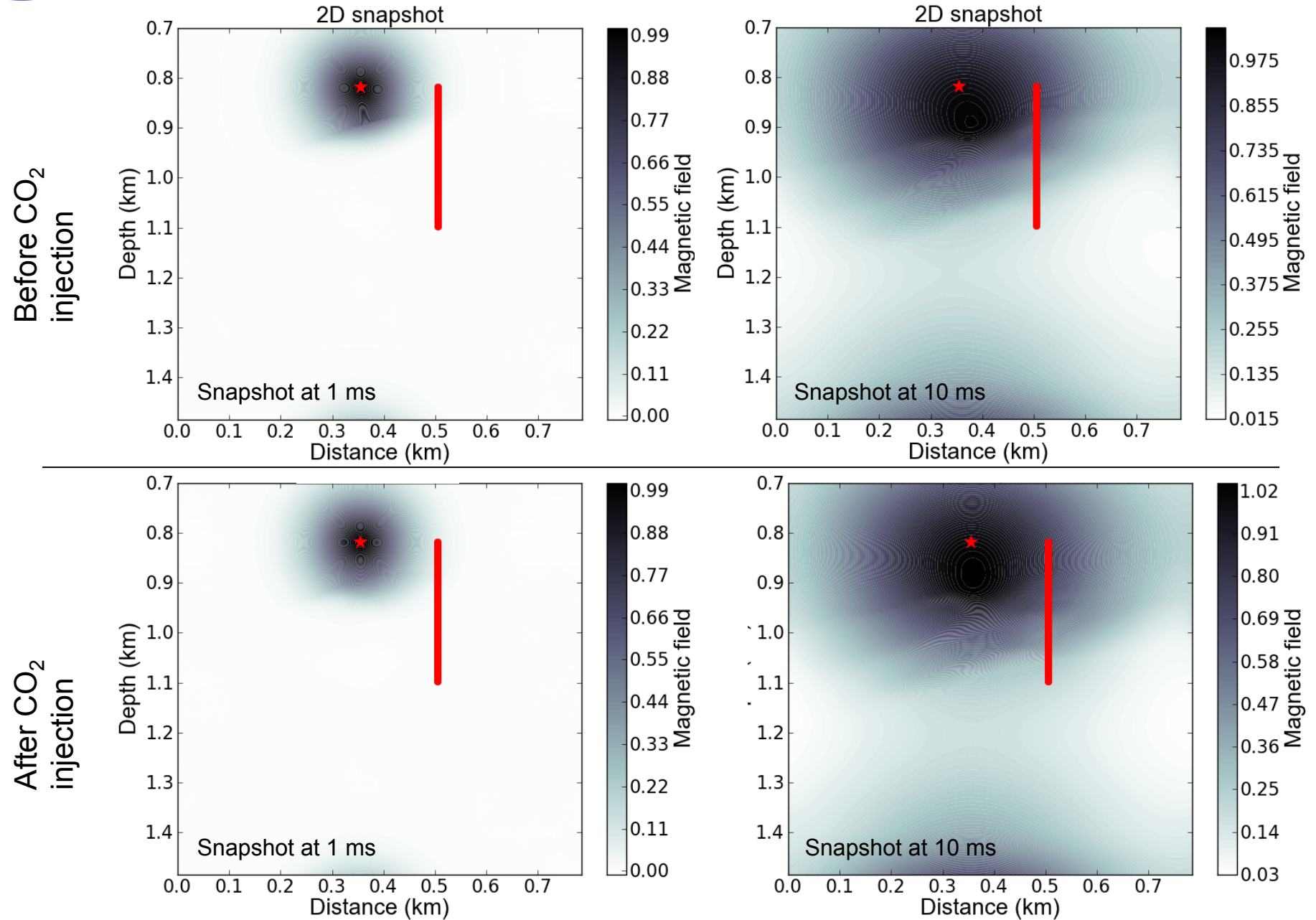
Boundary conditions: absorbing (sponge method)

Source time history: Dirac delta for H

(Carcione 2006, 2007, 2010)

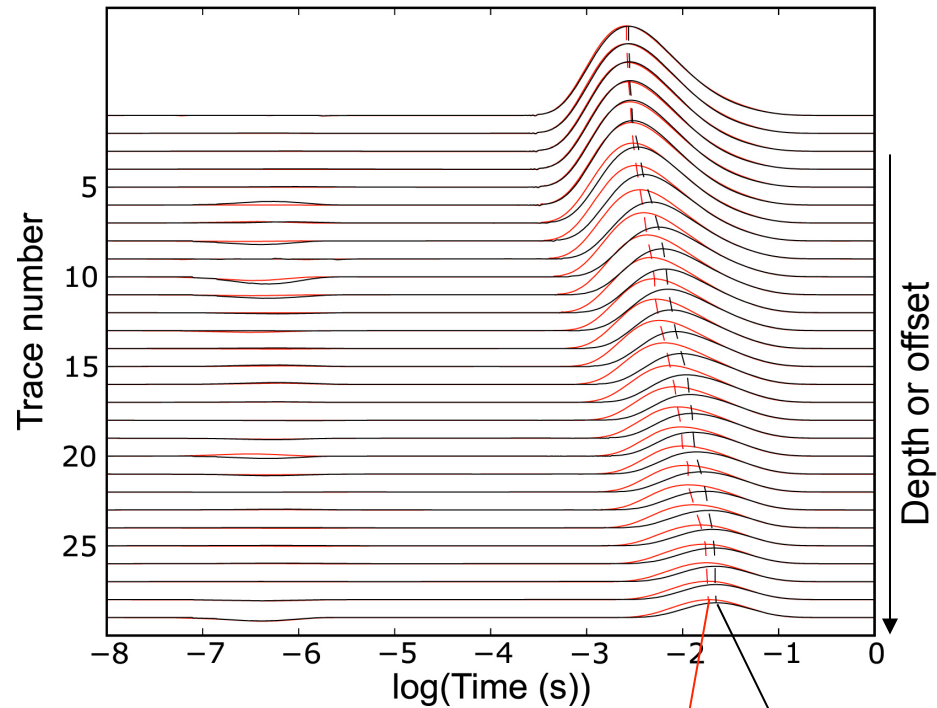


# EM numerical modelling



## EM before-after CO<sub>2</sub> injection

### Magnetic field



Black= before CO<sub>2</sub> injection

Red = after CO<sub>2</sub> injection

Picking of the maximum of the pulse:  
traveltimes of pre-injection data

Picking of the maximum of the pulse:  
traveltimes of post-injection data



## 2D viscoelastic wave equation

Newton's equations

$$\begin{aligned} \frac{\partial \sigma_{xx}}{\partial x} + \frac{\partial \sigma_{xy}}{\partial y} &= \rho \frac{\partial v_x}{\partial t} + f_x \\ \frac{\partial \sigma_{xy}}{\partial x} + \frac{\partial \sigma_{yy}}{\partial y} &= \rho \frac{\partial v_y}{\partial t} + f_y \end{aligned}$$

Constitutive equations

$$\begin{aligned} \frac{\partial \sigma_{xx}}{\partial t} &= (\lambda + 2\mu) \frac{\partial v_x}{\partial x} + \lambda \frac{\partial v_y}{\partial y} + (\lambda + \mu) \varepsilon_1 + 2\mu \varepsilon_2 \\ \frac{\partial \sigma_{yy}}{\partial t} &= \lambda \frac{\partial v_x}{\partial x} + (\lambda + 2\mu) \frac{\partial v_y}{\partial y} + (\lambda + \mu) \varepsilon_1 - 2\mu \varepsilon_2 \\ \frac{\partial \sigma_{xy}}{\partial t} &= \mu \left[ \left( \frac{\partial v_x}{\partial y} + \frac{\partial v_y}{\partial x} \right) + \varepsilon_3 \right] \end{aligned}$$

Memory variables equations

$$\begin{aligned} \frac{\partial \varepsilon_1}{\partial t} &= \frac{1}{\tau_\sigma^{(1)}} \left[ \left( \frac{\tau_\sigma^{(1)}}{\tau_\varepsilon^{(1)}} - 1 \right) \left( \frac{\partial v_x}{\partial x} + \frac{\partial v_z}{\partial z} \right) - \varepsilon_1 \right] \\ \frac{\partial \varepsilon_2}{\partial t} &= \frac{1}{2\tau_\sigma^{(2)}} \left[ \left( \frac{\tau_\sigma^{(2)}}{\tau_\varepsilon^{(2)}} - 1 \right) \left( \frac{\partial v_x}{\partial x} + \frac{\partial v_z}{\partial z} \right) - 2\varepsilon_2 \right] \\ \frac{\partial \varepsilon_3}{\partial t} &= \frac{1}{\tau_\sigma^{(2)}} \left[ \left( \frac{\tau_\sigma^{(2)}}{\tau_\varepsilon^{(2)}} - 1 \right) \left( \frac{\partial v_x}{\partial x} + \frac{\partial v_z}{\partial z} \right) - \varepsilon_3 \right] \end{aligned}$$

Material relaxation time

$$\tau_\varepsilon^{(v)} = \frac{\tau_0}{Q_v} \left[ \sqrt{Q_v^2 + 1} + 1 \right], \quad \tau_\sigma^{(v)} = \frac{\tau_0}{Q_v} \left[ \sqrt{Q_v^2 + 1} - 1 \right]$$

Regular grid (315 x 315; dx = dy = 2.5 m)

Spatial derivatives: pseudospectral (Fourier) method

Time evolution: fourth order Runge-Kutta scheme

Attenuation: viscoelastic model (Zener)

Boundary conditions: absorbing (sponge method)

Source time history: Ricker wavelet

$v_x, v_y$	= particle velocities
$\sigma_{xx}, \sigma_{yy}, \sigma_{xy}$	= stress component
$\rho$	= density
$f_x, f_y$	= body forces
$\varepsilon_1, \varepsilon_2, \varepsilon_3$	= memory variables
$\lambda, \mu$	= Lamé constants
$v_x, v_y$	= particle velocities
$\sigma_{xx}, \sigma_{yy}, \sigma_{xy}$	= stress component
$\rho$	= density
$f_x, f_y$	= body forces
$\varepsilon_1, \varepsilon_2, \varepsilon_3$	= memory variables
$\lambda, \mu$	= Lamé constants

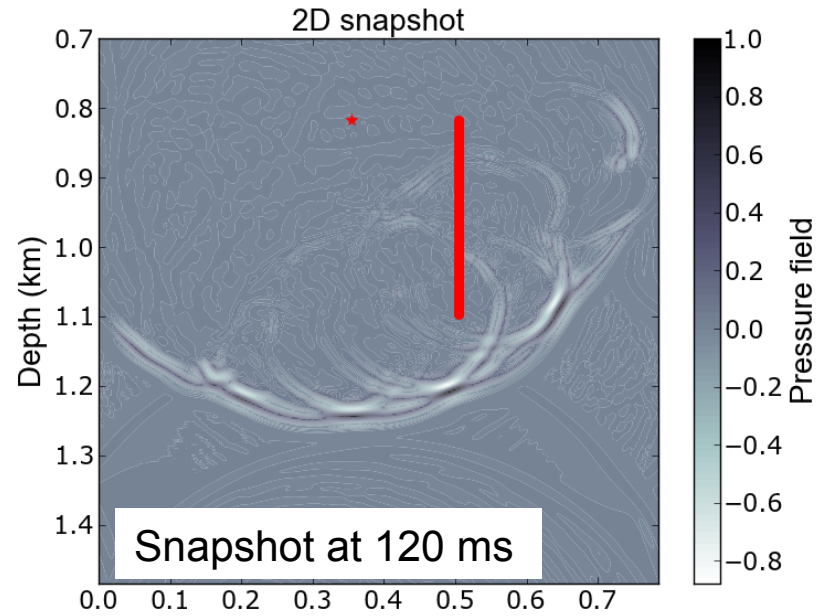
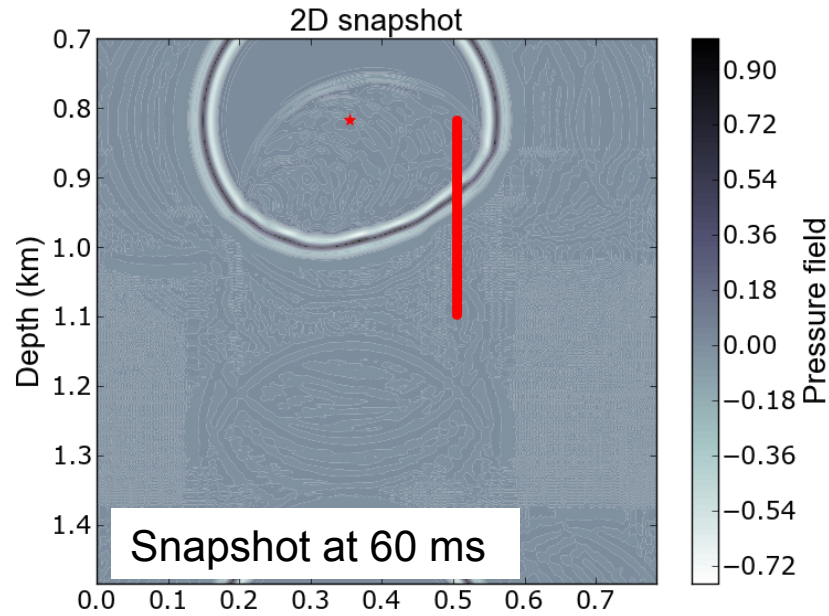


# Seismic numerical modelling

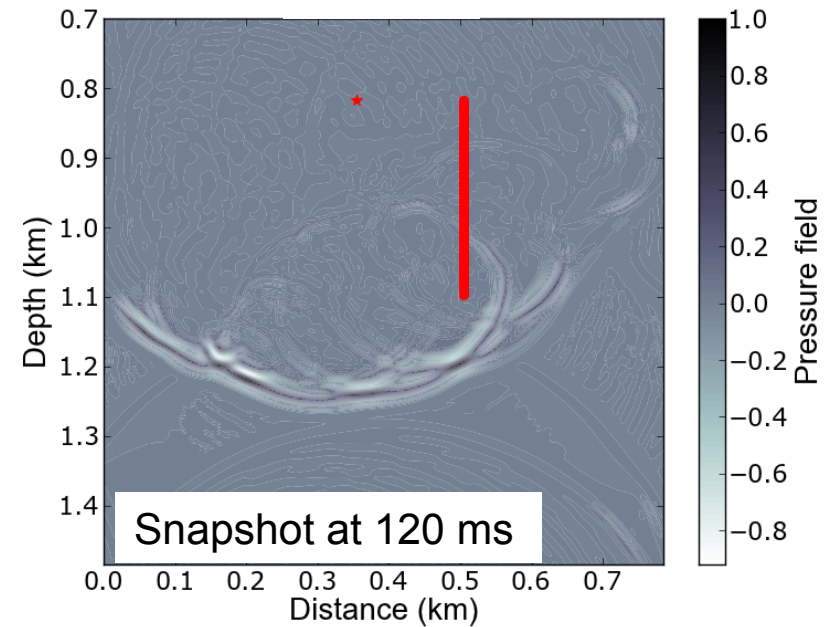
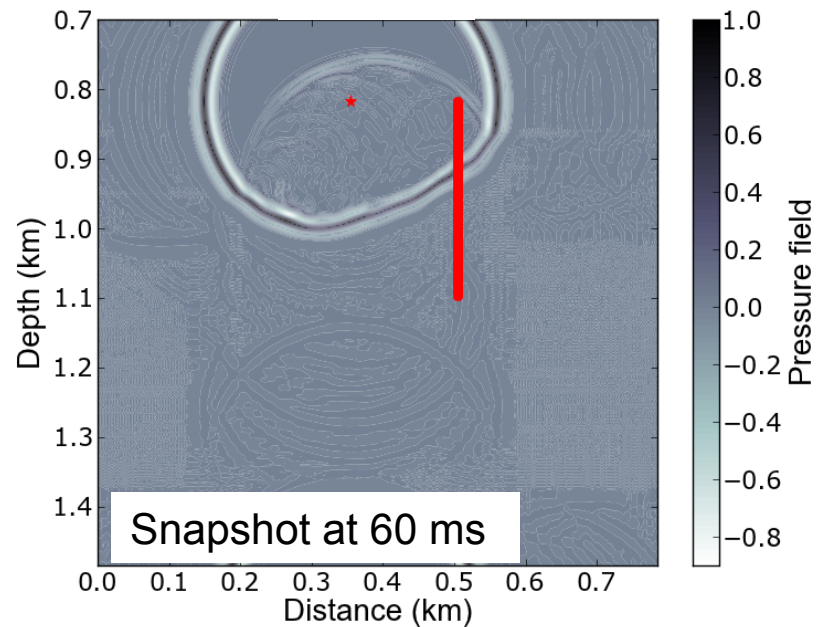


$f_p = 150$  Hz

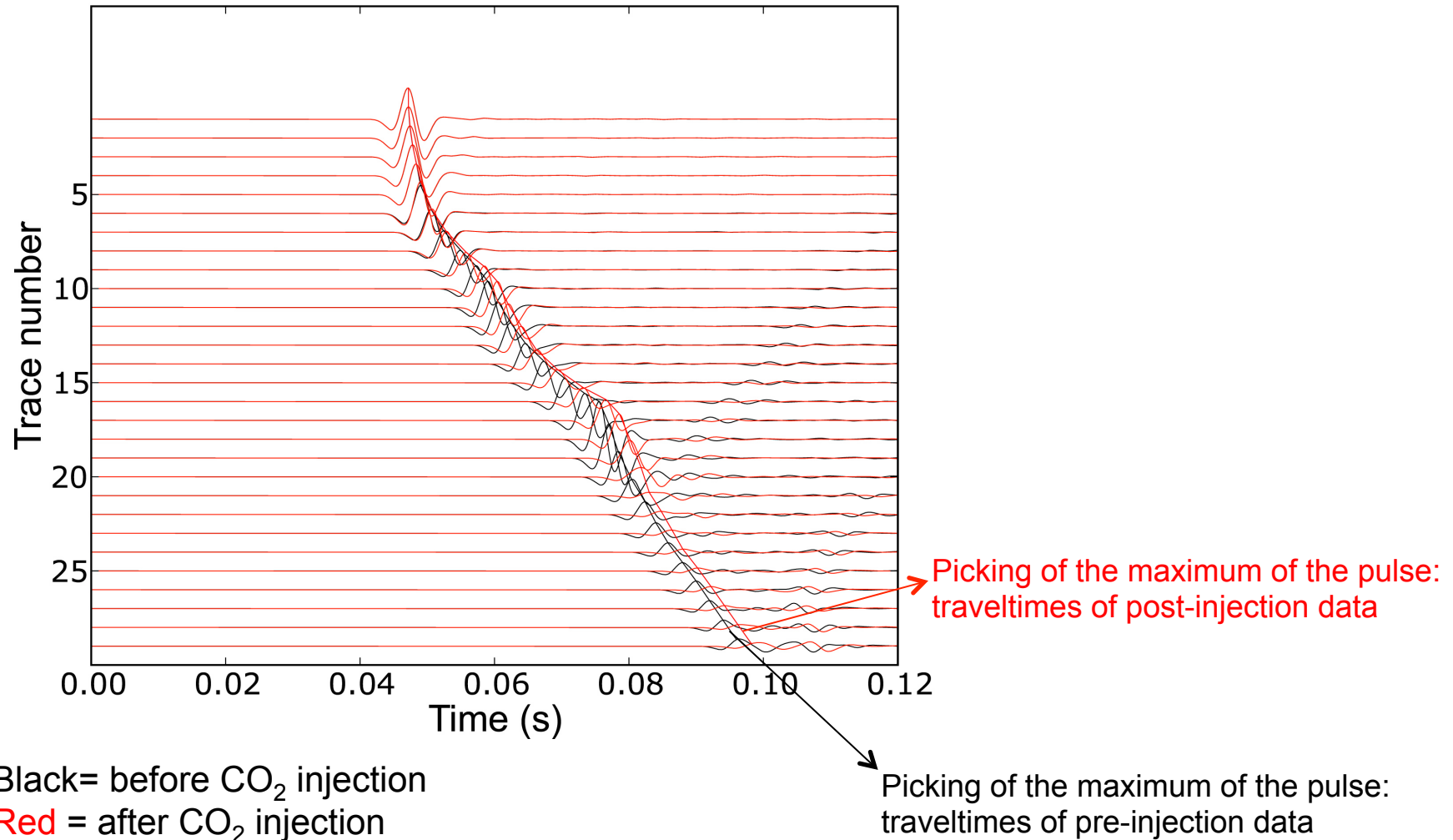
Before CO<sub>2</sub> injection



After CO<sub>2</sub> injection



## Seismic before-after CO<sub>2</sub> injection



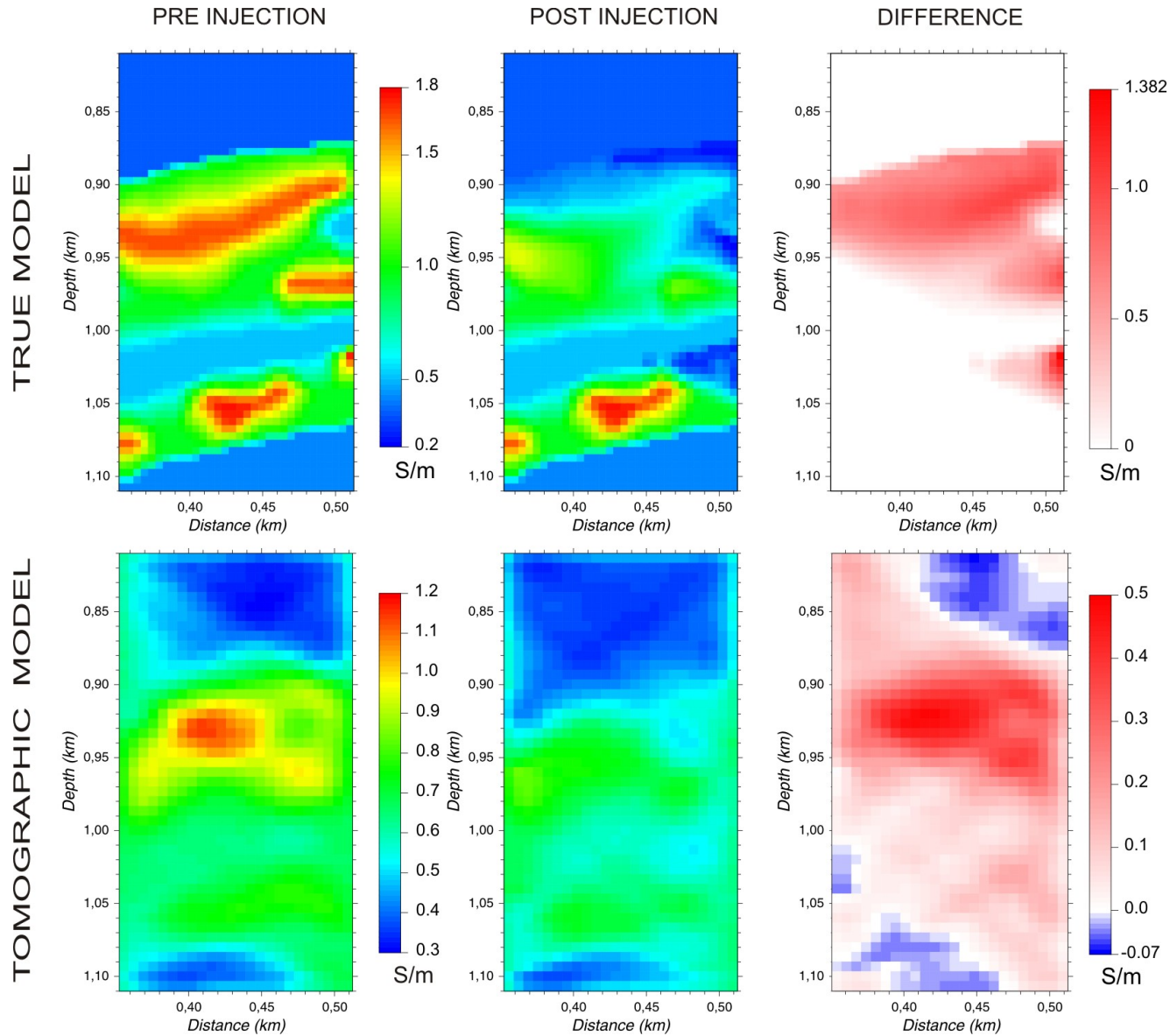




# Tomographic inversions



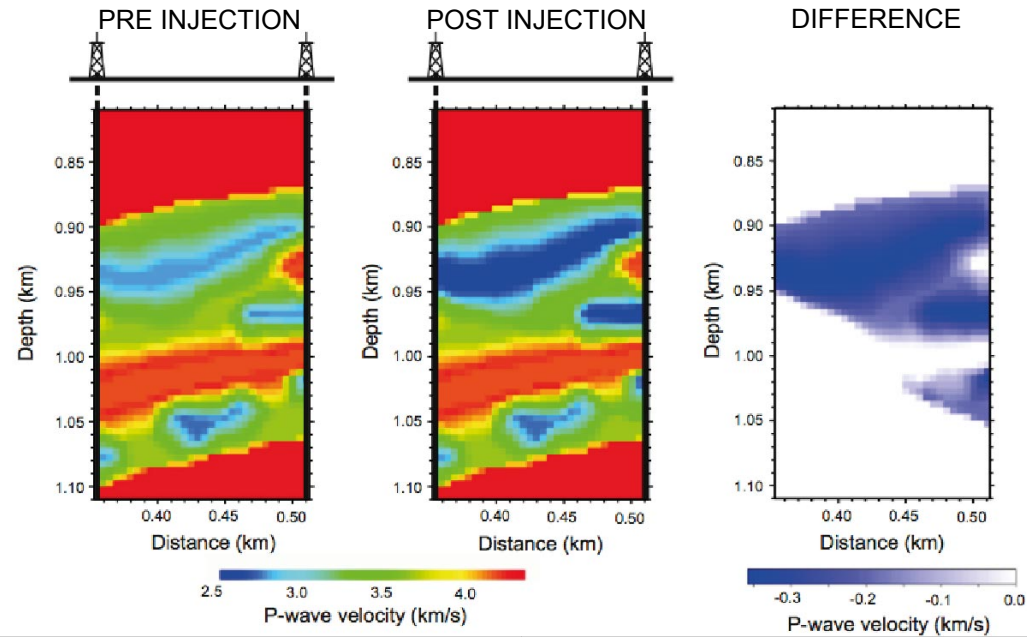
## EM tomography



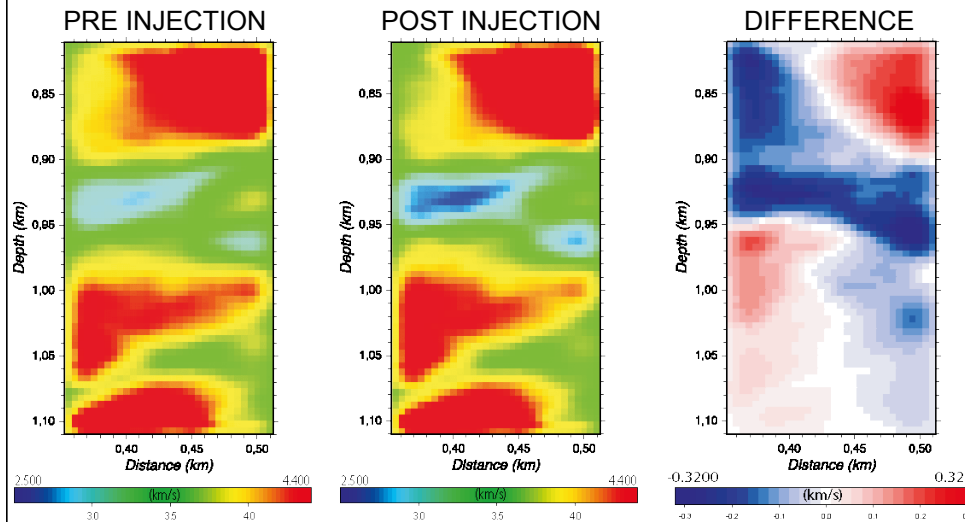


# Tomographic inversions

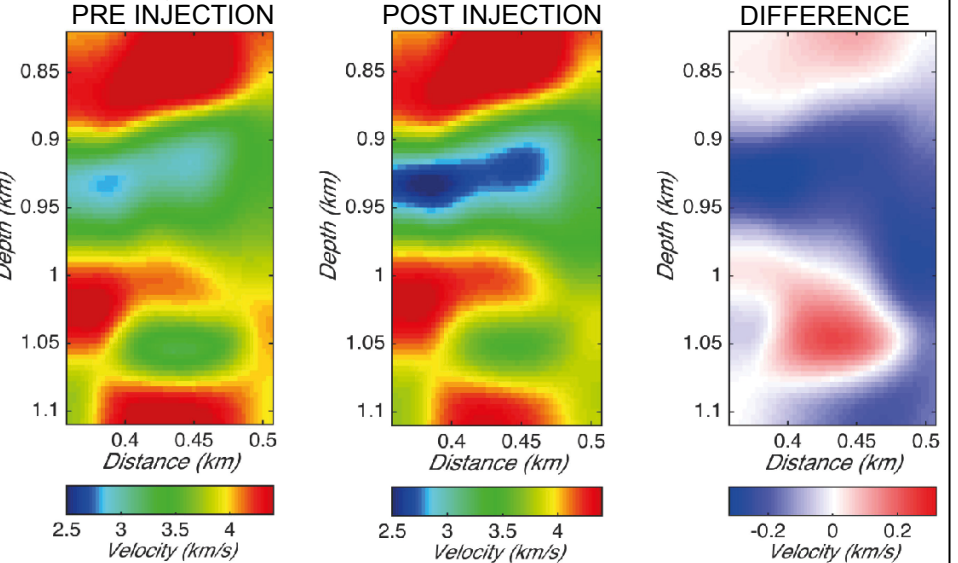
## P-wave tomography



### CAT – 3D



### Michellini, 1995

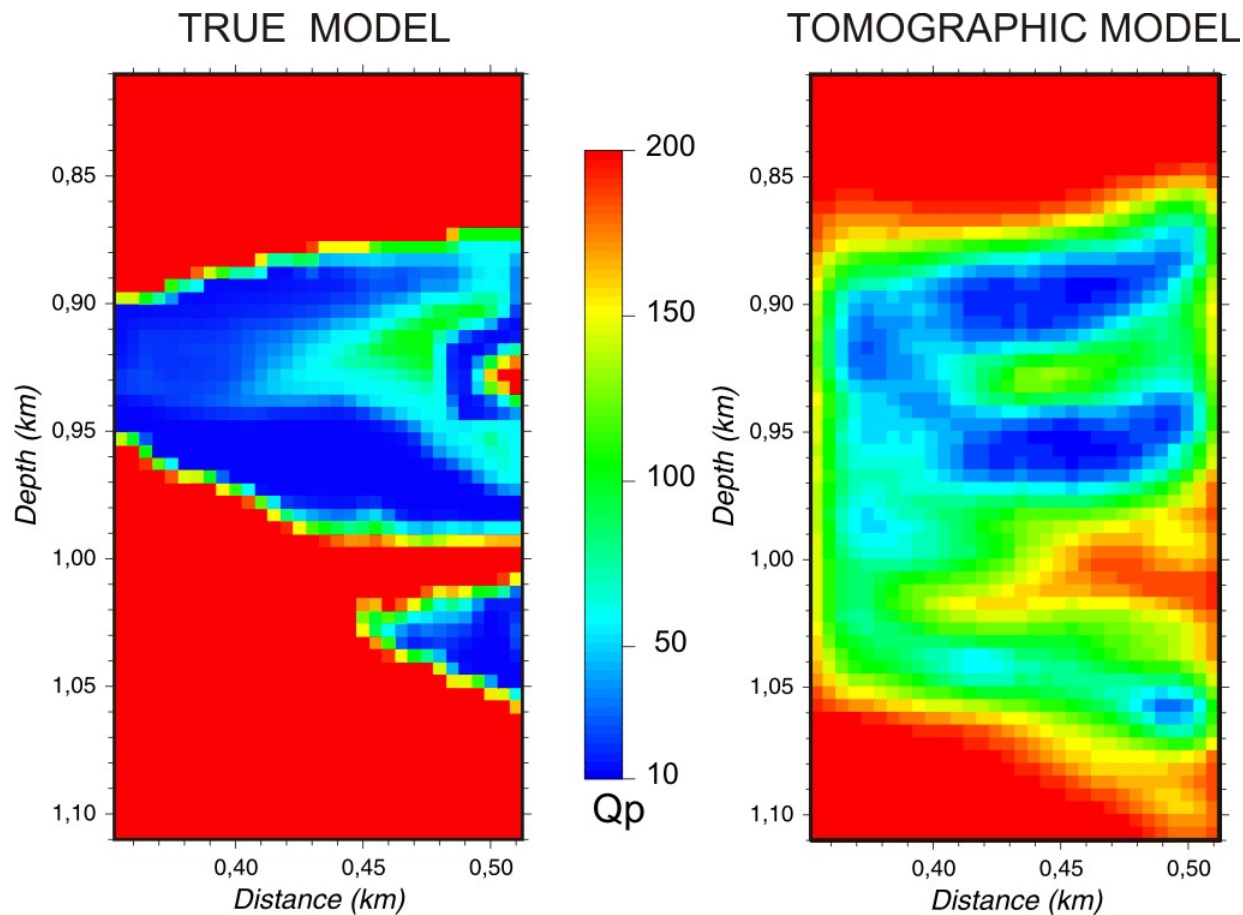




# Tomographic inversions



## P-wave quality factor





## Conclusions

- This study describes an effective methodology to monitor the injection of CO<sub>2</sub> in saline aquifers.
- The rock-physics models give reliable petrophysical properties of shaly sandstones partially saturated with CO<sub>2</sub>.
- Tomographic inversions of P-wave velocity,  $Q_p$  and electrical conductivity fields allow us to detect the presence of CO<sub>2</sub> after injection.

## Future work

- We are improving the methodology by considering saturation and pore pressure in the gas plume computed with fluid flow simulations.
- We are developing and testing a petrophysical inversion method using the tomographic results in order to obtain porosity, clay content and CO<sub>2</sub> saturation.